Vertical transport of tropospheric aerosols as indicated by 7 Be and 210 Pb in a chemical tracer model

JOURNAL OF GEOPHYSICAL RESEARCH, VOL. 101, NO. D13, PAGES 18,651–18,666, AUGUST 20, 1996

Vertical transport of tropospheric aerosols as indicated by ^{7}Be and ^{210}Pb in a chemical tracer model

Dorothy M. Koch[1]

Department of Geology and Geophysics, Yale University, New Haven, Connecticut

Daniel J. Jacob

Department of Earth and Planetary Sciences and Division of Applied Sciences, Harvard University, Cambridge, Massachusetts

William C. Graustein

Department of Geology and Geophysics, Yale University, New Haven, Connecticut

Abstract. We use the natural radionuclides ^{7}Be and ^{210}Pb as aerosol tracers in a three-dimensional chemical tracer model (based on the Goddard Institute for Space Studies general circulation model (GCM) 2) in order to study aerosol transport and removal in the troposphere. Beryllium 7, produced in the upper troposphere and stratosphere by cosmic rays, and ^{210}Pb, a decay product of soil-derived ^{222}Rn, are tracers of upper and lower tropospheric aerosols, respectively. Their source regions make them particularly suitable for the study of vertical transport processes. Both tracers are removed from the troposphere primarily by precipitation and are useful for testing scavenging parameterizations. In particular, model convection must properly transport and scavenge both ascending ^{210}Pb and descending ^{7}Be. The ratio $^{7}Be/^{210}Pb$ cancels most model errors associated with precipitation and serves as an indicator of vertical transport. We show that over land the annual average $^{7}Be/^{210}Pb$ ratio for surface concentrations and deposition fluxes vary little globally. In contrast, the seasonal variability of the $^{7}Be/^{210}Pb$ concentration ratio over continents is quite large; the ratio peaks in summer when convective activity is maximum. The model overestimates ^{7}Be in the tropics, a problem which we relate to flaws in the GCM parameterization of wet convection (excessive convective mass fluxes and no allowance for entrainment). The residence time of tropospheric ^{7}Be calculated by the model is 23 days, in contrast with a value of about 9 days calculated for ^{210}Pb, reflecting the high-altitude versus low-altitude source regions of these two tracers.

Introduction

Beryllium 7 and lead 210 are natural radionuclide tracers of aerosols originating over a range of altitudes in the atmosphere. Taken together, ^{7}Be and ^{210}Pb yield information on vertical motions in the atmosphere and the scavenging of aerosols. We investigate in this paper the factors controlling the atmospheric distributions of ^{7}Be and ^{210}Pb by using a global three-dimensional chemical tracer model (CTM) driven by meteorological output from a general circulation model (GCM) developed at the Goddard Institute for Space Studies (GISS).

The transport and persistence of tropospheric aerosols is a matter of growing concern, since anthropogenic sulfate contributions to the aerosol budget may play a significant role in recent climate changes [*Charlson et al.*, 1991, 1992]. Most of the aerosol optical depth is in the lower troposphere. However, *Clarke* [1992] found that formation of new particles (e.g., by SO_2 gas to particle conversion) is most likely to occur in the upper troposphere where the aerosol mass is low. Quantitative study of aerosol-climate relationships requires a GCM able to provide an adequate description of aerosols in all regions of the troposphere.

Several features make ^{7}Be and ^{210}Pb highly suitable tracers for improving GCM aerosol simulation. Their sources are known, global in extent, and relatively steady in time. Beryllium 7 ($t_{1/2}$=53 days) is produced by cosmic ray impact on nitrogen and oxygen

[1]Now at Columbia University, Goddard Institute for Space Studies, New York.

Paper number 96JD01176.
0148-0227/96/96JD-01176$09.00

atoms in the stratosphere and upper troposphere. Lead 210 ($t_{1/2}$=22 years) decays from ^{222}Rn ($t_{1/2}$=3.8 days) which is emitted from continents. Following production, they attach indiscriminately to available aerosols and are therefore spread evenly with respect to area over the ambient aerosol size distribution. They are chemically nonreactive, passive tracers, with radioactive half-lives that are long relative to the residence times of aerosols in the troposphere. They emit gamma radiation, which is easy to measure. Worldwide networks established to monitor nuclear activity have often measured ^{7}Be and ^{210}Pb activity as well. As a result, there is good global coverage of data, and many of the ^{7}Be records span two to three decades. Two types of observations are available: air concentrations (mostly taken at the surface) and deposition fluxes obtained from precipitation and seawater concentrations. Lead 210 was modeled previously in the (GISS) CTM by *Balkanski et al.* [1993, hereinafter referred to as B93]. Our study adds ^{7}Be to the model and utilizes the combination of ^{7}Be and ^{210}Pb.

The upper and lower atmospheric source regions of ^{7}Be and ^{210}Pb result in anticorrelations between the radionuclides where vertical transport processes are active. For example, convection pumps ^{222}Rn and ^{210}Pb upward and carries ^{7}Be downward. Dry convection is most active during the summer, producing summertime maxima in the ^{7}Be/^{210}Pb concentration ratio over continents. Convective scavenging, which is active in the tropics year-round and at higher latitudes during the summer over continents, produces asymmetries in removal since clouds tend to form over rising air leading to scavenging of upward moving species [*Giorgi and Chameides*, 1986; *Rodhe*, 1983]. B93 developed a parameterization in the CTM for scavenging aerosols in precipitating convective updrafts. This parameterization performs reasonably well for ^{210}Pb, which has relatively high concentrations near the surface. However, we will show that ^{7}Be concentrations are overpredicted by the model in regions where convection is active. This is a consequence of some combination of excessive downward transport and insufficient scavenging in convection. Thus the difference in the response of ^{7}Be and ^{210}Pb to convective transport and scavenging provides a new and powerful test for model convection parameterizations.

Numerous studies have used ^{7}Be measurements, usually in combination with other radionuclides, as an indicator of stratospheric influx [e.g., *Dibb et al.*, 1992, 1994; *Rangarajan and Gopalakrishnan*, 1970; *Rangarajan and Eapen*, 1990; *Sanak et al.*, 1985; *Viezee and Singh*, 1980]. It has also been recognized that tropospheric production may contribute to high ^{7}Be concentrations in surface air [e.g., *Dutkiewicz and Husain*, 1985]. Indeed *Feely et al.*, [1988] emphasized that ^{7}Be surface concentrations are influenced to varying degrees at different locations by stratosphere-troposphere exchange, precipitation scavenging, vertical transport in the troposphere, horizontal transport, and radioactive decay. We use the CTM, together with the information obtained from simultaneously modeling ^{210}Pb, to help distinguish between the importance of these factors on ^{7}Be concentrations and deposition at different locations. In particular, our study confirms the prominent role of convection in determining ^{7}Be (and ^{210}Pb) seasonality at midlatitude continental sites, as argued by Feely et al., [1988].

Beryllium 7 and ^{210}Pb were modeled by *Brost et al.*, [1991] and *Feichter et al.*, [1991], respectively, using the three-dimensional tracer model ECHAM2, which was developed from the European Centre for Medium Range Weather Forecasting (ECMWF) model. These studies used a first-order scavenging parameterization [*Giorgi and Chameides*, 1986] for both convective precipitation and large-scale precipitation. The lack of precipitation scavenging within convective cloud updrafts resulted in ^{210}Pb surface concentrations which were at least 40% higher than measured values, while deposition fluxes were underestimated. Agreement for ^{7}Be was much better. They did not make extensive use of the combination of ^{210}Pb and ^{7}Be, although they commented on the utility of such a study. *Rehfeld and Heimann* [1995] used the ECMWF model to simulate ^{210}Pb, ^{7}Be, ^{10}Be, and ^{90}Sr. They also used a first-order scavenging parameterization but were more successful than *Feichter et al.* [1991] at simulating ^{210}Pb surface concentrations (the root mean square value between observations and model was about 0.2 mBq/m^3 STP [*Rehfeld*, 1994]). The model version used by *Rehfeld and Heimann* [1995] incorporates observed meteorological winds and precipitation from 1990, and they compared model results with ^{7}Be and ^{210}Pb data collected in 1990. In contrast, we use 1 year's output from the GISS GCM 2, which generates internally consistent climatology, and we compare results with observations averaged over all available years.

Beryllium 7 Source

We will confine our discussion to the ^{7}Be source, since the ^{210}Pb source is described by B93. Beryllium 7 is generated by cosmic rays, which travel along magnetic field lines, so that the source is strongest near the poles (see Figure 1). The cosmic rays collide with atoms in the upper atmosphere, generating a cascade of neutrons and protons, which in turn interact with nitrogen and oxygen atoms, resulting in ^{7}Be production. The encounter of the neutrons and protons with the nitrogen and oxygen atoms is called spallation or "star" production. The magnitude of ^{7}Be production is a trade-off between the energy level of the bombarding particles and the density of the atmospheric N and O targets, so that maximum production occurs in the stratosphere (Figure 1). Very soon after production, ^{7}Be attaches to available aerosol particles. ^{7}Be production has neglible dependence on season or longitude.

In addition to the dependence of production on altitude and latitude, production also varies with the $\approx$ 11-year solar cycle. When solar activity is high, cosmic rays are deflected away from the solar system, and ^{7}Be production decreases. Figure 2 shows annual average

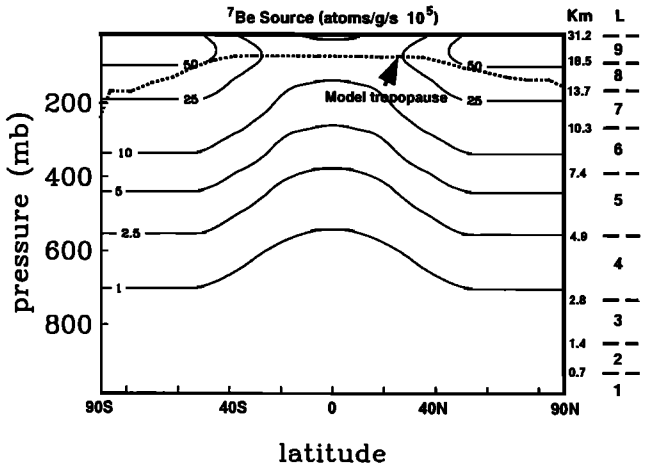

Figure 1. Beryllium 7 source [*Lal and Peters*, 1967]. Atmospheric pressure is shown in the left margin, and the altitudes of the general circulation model (GCM) layers are shown in the right-hand margin. Also shown is the annual average tropopause height in the GCM (dashed line) (Y. J. Balkanski, personal communication, 1994). The units are ^{7}Be atoms s^{-1} (gram of air)$^{-1}$ $\times$ 10^5.

^{7}Be concentrations at four sites with long data records. Figure 2 also shows the annual average Wolf sunspot series, an indicator of solar activity, which are anticorrelated with ^{7}Be [*Koch and Mann*, 1996]. The amplitude of ^{7}Be surface concentration variability related to the solar cycle is about 20-25% from the mean, as shown in Figure 2, a value consistent with previous studies. *O'Brien et al.* [1991] (e.g., their Table 2) calculated about 42% variation in star production rate between solar minima and maxima. *Lal and Peters* [1967] show the cosmic ray intensity ratio between the solar maximum year 1958 and a minimum year 1954 as a function of atmospheric pressure and latitude (their Figure 15). At 48° latitude and 200 mbar, this difference is about 40%.

The ^{7}Be source has been derived using both observations [*Lal and Peters*, 1967 (hereinafter referred to as LP67)] and calculations [*O'Brien*, 1979; *O'Brien et al.*, 1991] of star production and of the yield of ^{7}Be atoms per star ("cross section"). The source given by LP67 is based on observations made during the solar maximum (low ^{7}Be production) year of 1958. This source is about 50% larger than the solar maximum source given by *O'Brien et al.* [1991]. The LP67 cross section also happens to be 50% larger than that calculated by *O'Brien et al.* [1991], and this difference may explain the discrepancy between the sources. Since the *O'Brien et al.* [1991 source yields model concentrations at the surface and within the stratosphere which are much lower than observed, we have used the LP67 source (Figure 1).

To use ^{7}Be data from different years, we corrected all data to the 1958 solar maximum source used in the model. To make the correction, we chose 15 sites which have long data records, $\mathbf{b}_i(t)$, where i is the site and t spans 15-20 years of data. Data at each site was normalized and demeaned using the average value $< \mathbf{b}_i(t) >$ at that site, and the sunspot time series $\mathbf{x}(t)$ was also normalized and demeaned by its average value $< \mathbf{x}(t) >$. The normalized amplitude of ^{7}Be variability is not noticeably affected by elevation or latitude. We calculated regression coefficients m_i between the sunspot series and each ^{7}Be data record:

$$m_i = \frac{\mathbf{x}'(t) \cdot \mathbf{b}'(t)_i}{\mathbf{x}'(t)_i \cdot \mathbf{x}'(t)_i}, \tag{1}$$

where the primes indicate the normalized demeaned series. We then averaged the m_i, using those records which had f-test significance values greater than 75% (some sites appear to be greatly affected by other factors, so that the solar signal was less noticeable) to get m. The correlation increased during the most recent solar cycle. If only the years 1980-1992 were used, the average regression coefficient was $m = -0.25$, but the entire records (about 1970-1992) gave $m = -0.19$. The increase in m may result from the stronger solar modulation during the most recent cycle relative to the previous cycle (1970-1980) [*Koch and Mann*, 1996] (Figure 2). We used the lower value to correct the data before 1980 and the larger value for more recent data. The corrected values β_j are given by

$$\beta(t)_j = \mathbf{b}(t)_j - m\mathbf{x}'(t) < \mathbf{b}(t)_j >, \tag{2}$$

where j represents the entire data set and the angle brackets indicate the mean value at the respective site. Having corrected all data to an average solar year value, we then multiply by 0.72 to correct to the 1958 solar maximum source. This 28% reduction is larger than the average departure from the mean because the difference in production rate (or solar activity) between the very large 1958 solar maximum and an average solar year is greater than between a solar minimum year and the average solar year.

We found that ^{7}Be model results are highly sensitive to the simulation of the tropopause, and adjustment was required to correct for excess flux from the stratosphere to the troposphere in the GCM. Since our primary interest is in simulating the behavior of ^{7}Be in the troposphere, this is a way of adjusting the upper boundary condition for the study region. C.

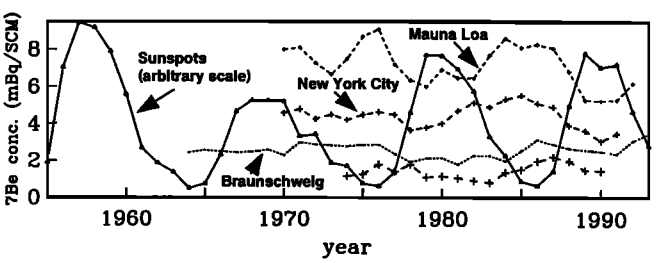

Figure 2. Observed annual average concentrations as a function of year from (top to bottom) Hawaii, New York City, Braunschweig, Germany, and Skibotn, Norway. Solid line connects the annual average Wolf sunspot number (from *National Geophysical Data Center*) as a function of year. The sunspot number is an index of solar activity.

M. Spivakovsky (personal communication, 1994) found that stratosphere-troposphere exchange in the model is about twice the amount required to accurately simulate ^{14}CO from bomb fallout. To compensate for the high flux into the troposphere, we decreased the ^{7}Be flux by a factor of 2 in the top two layers of the CTM. This adjustment significantly improved the ^{14}CO surface concentration simulations at all latitudes (C. M. Spivakovsky, personal communication, 1994), and also improves the ^{7}Be simulation. The ^{7}Be deposition flux is particularly sensitive to changes in flux across the tropopause and to tropopause location, as also shown by *Tanaka and Turekian* [1995].

In this model, about 40% of the tropospheric ^{7}Be was generated in the stratosphere. This value is higher than that derived by *Dutkiewicz and Husain* [1985] based on ^{7}Be surface concentrations and bomb-derived ^{90}Sr concentrations; however, it is consistent with their findings at higher altitudes in the troposphere. Dutkiewicz and Husain found a seasonal variability of stratosphere-generated ^{7}Be ranging from about 10% in fall to about 40% in spring at midlatitude continental surface sites. The model has a much smaller amplitude of variability at midlatitudes, with about 36% stratospheric contribution to surface concentrations in summer/fall and 40% in winter/spring. However, with only one to two model layers in the stratosphere we do not expect to accurately simulate stratosphere-troposphere exchange.

Model Description

The CTM is driven by 1 year of archived meteorological output from the GISS GCM (model 2) [*Hansen et al.*, 1983]. Horizontal resolution is 4°x5° (latitude x longitude), with nine vertical layers (see Figure 1). The CTM time step is 4 hours, and most of the required GCM output is archived in 4-hour intervals (surface pressure, wind velocity, mixed layer depth, convective and large-scale precipitation within the column, and cloud optical depth). Further details are given by *Prather et al.* [1987] and subsequent studies referenced by B93.

The ^{7}Be source was constructed by fitting cubic splines to production values provided by D. Lal (personal communication, 1994) (shown in Figure 1) and computing the average ^{7}Be production within each model layer as a function of latitude. Because of the large changes in production with altitude we calculated and used first-order vertical moments of the source as described by *Prather* [1986].

The GCM and CTM distinguish between large-scale precipitation, shallow wet convection (events confined below layer 4), deep wet convection, and dry convection. The vertical distribution of convective events and large-scale precipitation is archived from the GCM as 5-day averages, so that event heights are reconstructed in the CTM by combining this information with the 4-hour archives of event occurrences. For dry convective events, when air is unstable with respect to the dry adiabat, the unstable column is mixed uniformly. For wet convective events, when air within the column is unstable with respect to the wet adiabat, 50% of the air in the lowest grid box is moved upward to the point where its density is in equilibrium with the environment and is deposited in that layer, followed by subsidence of dry air within intermediate layers as required to conserve mass. The scheme then checks each layer above for instability; however, 50% mass flux is generally far greater than is required to stabilize the column. This GCM version did not include cloud entrainment, anvil precipitation, or cloud downdrafts.

B93 employed a wet convection scavenging parameterization consistent with the vertical mass flux occurring in the GCM convective events. A given percentage of aerosol is removed from the upward moving air for all wet convective events. B93 used 100% removal for deep convective events and 50% removal for shallow convection. While this procedure was reasonably successful for simulating ^{210}Pb, we found that it resulted in excessive ^{7}Be surface concentrations in the tropics and in the summers at midlatitudes. One reason for this is that scavenging only occurs within air moving upward in the updraft, i.e., in air originating in the lowest convective layer, since convection in this GCM is nonentraining. Hence this mechanism efficiently removes ^{210}Pb relative to ^{7}Be because a much larger percentage of the ^{210}Pb inventory exists in the lower troposphere. The model also does not account for scavenging in the cloud anvil, or the laterally sheared cloud top. To compensate for these model deficiencies, we applied a first-order rainout parameterization to regions of convective precipitation in addition to the convective scavenging parameterization of B93. We will show that this added scavenging improves the simulation in the tropics for both ^{7}Be and ^{210}Pb.

The *Giorgi and Chameides* [1986] first-order rainout parameterization is used for both large-scale and convective precipitation, in addition to the scavenging in wet convective updrafts described by B93. The fraction of the grid box experiencing precipitation is given by

$$F = \frac{F_0 Q \Delta t / T_c}{Q \Delta t / T_c + F_0 \beta L}, \tag{3}$$

where Q is the model-derived mean water condensation rate, $\Delta t = 4$ hours is the model time step, L is the cloud liquid water content ($L = 2 \times 10^{-3}$ kg m^3 for convective and $L = 0.5 \times 10^{-3}$ kg m^3 for large-scale precipitation), and F_0 is the maximum value of F (=0.3 for convective and 1 for large-scale precipitation). The value of the precipitation duration T_c is chosen to maximize agreement between CTM and observed precipitation frequencies (=2 and 4 hours for convective and large-scale precipitation) (B93). The frequency of cloud water to rainwater conversion β, which is also the exponential rate constant of aerosol removal for scavenging within the cloud (rain-out), is

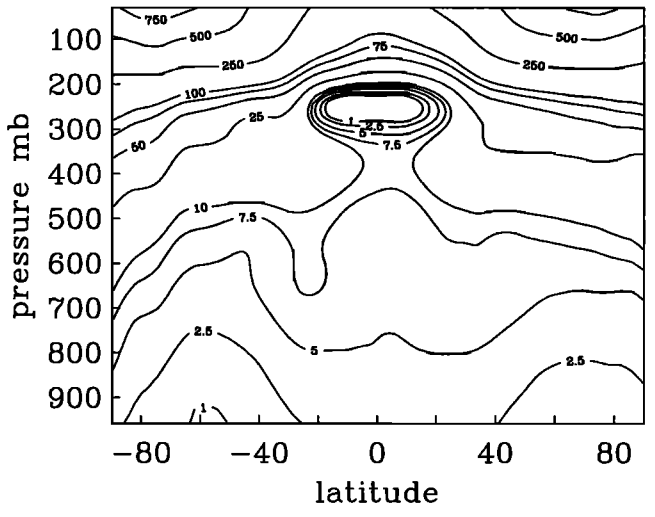

Figure 3. Annual, zonal average of model ^{7}Be concentrations (mBq/m^3 STP).

$$\beta = \frac{Q\Delta t}{FLT_c} \tag{4}$$

for large-scale precipitation but is fixed at $\beta = 1.5 \times 10^{-3}s^{-1}$ for convective precipitation. Rain-out is shut off when the temperature is less than T = 258 K, to represent precipitation formation in the absence of riming [*Davidson*, 1989]. For below-cloud scavenging, or washout, we use a rate constant of 0.1 mm^{-1} normalized to the precipitation rate in the precipitating fraction F of the grid box [*Dana and Hales*, 1976; B93].

Comparison of Model With Observations

Zonal Concentration Profiles

Figure 3 shows the zonal annual average ^{7}Be concentration generated by the model. Very low concentrations are found in the upper troposphere in the tropics, reflecting the frequent injection of lower tropospheric

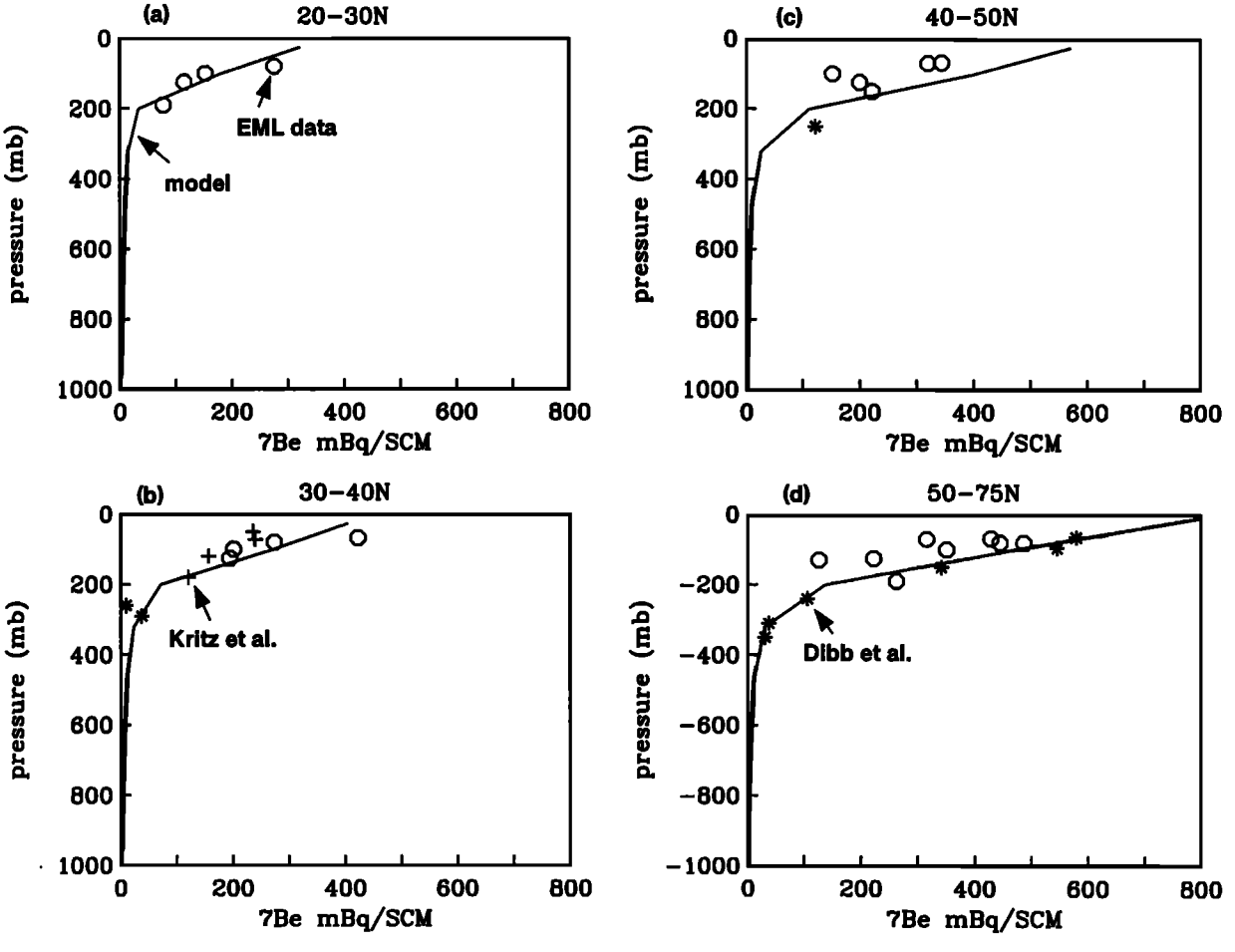

Figure 4. Comparison of model annual zonal average ^{7}Be profiles with high-altitude data for four latitude bands: (a) 20°-30°N, (b) 30°-40°N, (c) 40°-50°N and (d) 50°-75°N. Circles are from Environmental Measurements Laboratory [*Leifer and Juzdan*, 1986], pluses are from *Kritz et al.* [1991], and asterisks are from *Dibb et al.* [1994]. Model results are shown as lines. Units are mBq/m^3 STP.

air in wet convective updrafts from which aerosol is efficiently scavenged. The dry descending limbs of the Hadley cells show relatively high ^{7}Be concentrations in the midtroposphere of the subtropics. Subsidence over the south pole also elevates concentrations there.

Since most ^{7}Be production occurs at high altitudes, we use stratospheric measurements to verify the source. Although the data are sparse, stratospheric concentrations should remain relatively constant. In Figure 4 we compare model-generated annual average ^{7}Be concentration profiles with data from the Environmental Measurements Laboratory (EML) [*Leifer and Juzdan*, 1986], from *Kritz et al.* [1991] and from *Dibb et al.* [1994] (including some taken from previous studies) for four different latitude bands. Overall agreement between model and observations is good, giving credibility to both the LP67 source and our solar cycle correction.

Deposition Fluxes

The GCM is intended to simulate a typical meteorological year, rather than a specific year; evaluation of model results with observations must therefore focus on long-term statistics rather than on measurements for any specific day.

Young and Silker [1980] have compiled an extensive data set of ^{7}Be inventories in the mixed layer of the Pacific and Atlantic Oceans. These inventories can be viewed as representing a steady state between atmospheric deposition and radioactive decay and serve therefore as an estimate of the deposition flux. In Figure 5 we compare our simulated annual mean inventories of deposited ^{7}Be (Figure 5a) to the data of *Young and Silker* [1980] (Figure 5b). As pointed out by Young and Silker, much of the deposition flux spatial pattern

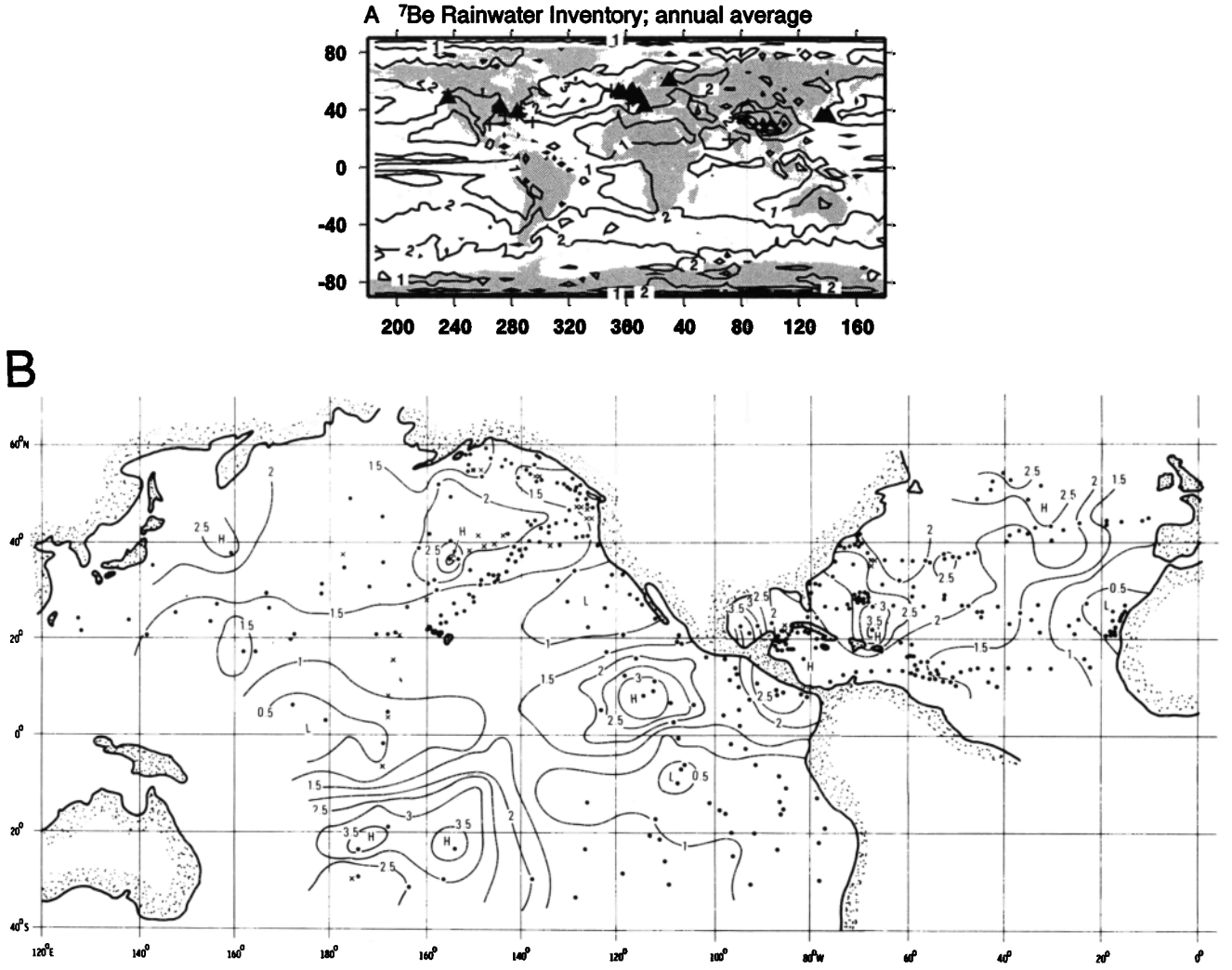

Figure 5. (a) Modeled ^{7}Be inventory in rainwater. Locations shown for ^{7}Be deposition flux sites (triangles) and for sites with both ^{7}Be and ^{210}Pb (pluses). Deposition sites are taken from *Baskaran et al.* [1993], *Bleichrodt* [1978] (and references within), *Brown et al.* [1989], *Crecelius* [1981], *Dibb* [1989], *Hasebe et al.* [1981], *Knies* [1994], *Lal et al.* [1979], *Olsen et al.* [1985], *Todd et al.* [1989], and *Turekian et al.* [1983]. (b) Observed ^{7}Be inventory reprinted from *Earth and Planet. Sci. Lett.*, 50, *Young and Silker*, Aerosol deposition velocities on the Pacific and Atlantic Oceans calculated from ^{7}Be measurements, 92-104, 1980, with kind permission of Elsevier Science - NL, Sara Burgerhartstraat 25, 1055 KV Amsterdam, The Netherlands. Figures 5a and 5b have a contour interval of 1.0 and 0.5 dpm/cm^{2}, respectively.

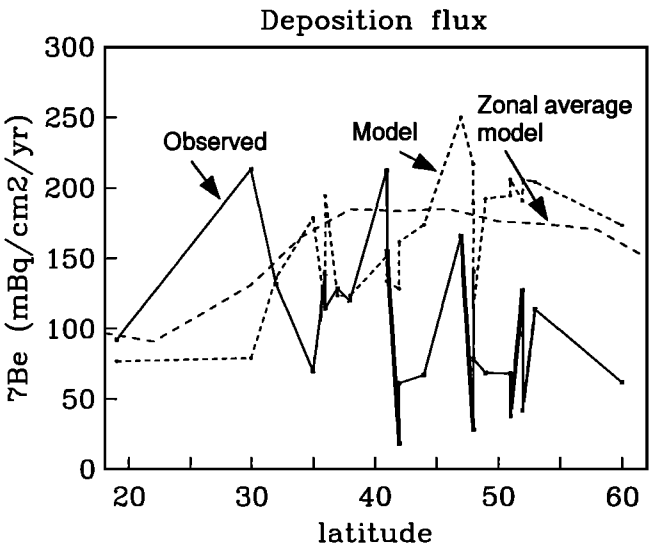

Figure 6. Annual mean deposition flux of ^{7}Be (mBq/cm^2/yr) at sites shown in Figure 11 as a function of latitude. The solid line connects observations and the short-dashed line connects model values. The long-dashed line is the zonal average model deposition flux.

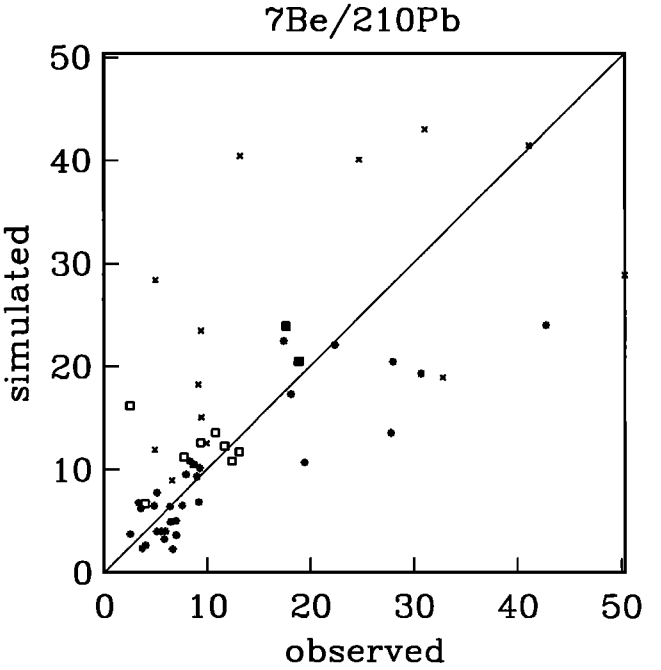

Figure 7. Scatterplot comparing model and observed ratio of ^{7}Be to ^{210}Pb. Deposition flux is shown by open squares, and marine sites by solid squares. The surface concentration locations are distinguished between low-elevation continental sites (asterisks) and remaining sites (crosses).

can be explained by precipitation amount. The model agreement is generally good. For example, the low-flux regions to the west of North America, South America, and Africa have the right location and magnitude. The high-flux regions in the northwestern Atlantic and Pacific Oceans are placed nearly correctly in the model. However, the observed maxima in the eastern equatorial Pacific and the south central subtropical Pacific are underestimated by the model.

Long-term records of ^{7}Be deposition flux (1 year or longer) are available from 25 northern midlatitude sites (Figure 5a). Figure 6 compares the simulated and observed deposition fluxes at the individual sites. Also shown is the zonal average model deposition flux. Figures 5 and 6 show that the model overpredicts deposition flux at high latitudes.

We define mean model bias γ as

$$\gamma(j) = \frac{\sum(\text{model}(j) - \text{observation}(j))}{\sum \text{observation}(j)}, \qquad (5)$$

where j could be ^{7}Be, ^{210}Pb, or ^{7}Be/^{210}Pb; $\gamma = 0$ means zero mean bias. The overall model bias for the ^{7}Be deposition flux, based on the data shown in Figure 6, is $\gamma(^7\text{Be}) = 0.61$. Without the stratosphere-troposphere flux adjustment described in the previous section, this value would be $\gamma(^7\text{Be}) = 0.81$. In comparison, the mean bias for ^{210}Pb deposition flux reported in B93 was close to zero; however, B93 used a larger number of ^{210}Pb sites.

Figure 7 compares simulated and observed annual mean ratio of ^{7}Be and ^{210}Pb deposition fluxes. Here and elsewhere we first calculate the model temporal average ^{7}Be and ^{210}Pb and then take the ratio, in order to be comparable with the observations. The bias of the deposition flux ratio is only $\gamma(^7\text{Be}/^{210}\text{Pb}) = 0.29$ but was 0.47 without the tropopause flux adjustment. The improvement over ^{7}Be occurs because GCM precipitation anomalies, which affect ^{7}Be and ^{210}Pb in a similar manner, are reduced in the ratio. The two highest ^{7}Be/^{210}Pb deposition flux ratios are at Bermuda and Mace Head, Ireland (solid squares), which receive mostly marine air and have relatively low ^{210}Pb deposition flux. The remaining points (open squares) are continental and have lower ratios.

Surface Air Concentrations

Long-term records of ^{7}Be concentrations in surface air are available from 70 sites around the world, shown in Figure 8 (pluses are sites with ^{210}Pb and ^{7}Be; triangles are ^{7}Be only). Figure 8 also shows contours of the annual average model ^{7}Be surface concentration. The model surface concentrations are maximum near the equator and over continents. The higher concentrations over continents are due both to higher elevation and to dry convection [*Young and Silker*, 1980; *Uematsu et al.*, 1994], as discussed further below (section 5.1).

In Figure 9 we compare model and observed annual average ^{7}Be surface concentrations at each site, as a function of latitude. The model zonal average is also shown. The observations tend to be highest in the subtropics and at midlatitudes. Much of the local variability in the observations results from the tendency for concentrations to be greater at high elevations and

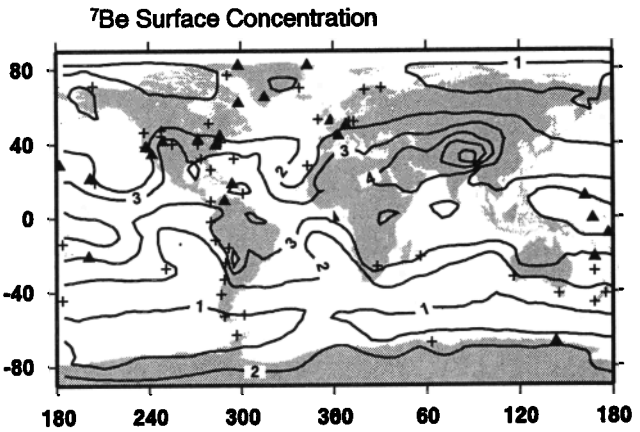

Figure 8. Locations of surface air concentration data: pluses are sites with both ^{210}Pb and ^{7}Be; triangles are ^{7}Be only. Annual average ^{7}Be surface concentration calculated in the model is shown by contours with 1 mBq/m^3 STP intervals. Data are taken from *Dibb et al.* [1994] (Alert, Canada), *Dutkiewicz and Husain* [1985] (Whiteface Mountain), *Kolb* [1992] (Vardo, Skibotn, Braunschweig, Berlin), *Lambert et al.* [1990] (Dumont D'Urville), *Marenco and Fontan* [1974] (Toulouse), *Parker* [1962] (Sutton), *Uematsu et al.* [1994] (Midway, Oahu, Enewetak, Nauru, Funafuti, Samoa, Raratonga, New Caledonia), *Schumann and Stoeppler* [1963] (Heidelberg), Shapiro and Forbes-Resah [1976] (Fullerton), and K. K. Turekian and W. C. Graustein (unpublished data, 1994) (Mace Head, Bermuda, Izania, Barbados, New Haven, Santa Rosa, Champaigne). Remaining sites are from the Environmental Measurements Laboratory [*Feely et al.*, 1981, 1985, 1988, *Larsen and Sanderson*, 1990, 1991, and R. J. Larsen, personal communication, 1995].

over continents. The global average of observed surface concentration is 2.45 mBq/m^3 STP; the average of those sites with elevations greater than 700 meters is 3.54 mBq/m^3 STP, and the average of the (low elevation) coastal and ocean sites is 1.84 mBq/m^3 STP. The model overestimates the concentrations in the tropics and is somewhat low at northern hemisphere midlatitudes. We can use ^{210}Pb and ^{7}Be/^{210}Pb to help determine whether these biases are related to model errors in transport or in precipitation scavenging.

The biases for ^{7}Be, ^{210}Pb, and ^{7}Be/^{210}Pb surface concentrations, as defined in equation (5), are given in Table 1 for low latitudes (< 20°), high latitudes (> 20°), and for all sites. Our average bias for ^{210}Pb is lower than the value reported by B93, which was close to zero. This is due mostly to the use of a different set of sites.

In the tropics we expect that most ^{7}Be and ^{210}Pb should be removed by wet convective scavenging. However, both ^{7}Be and ^{210}Pb are overestimated by the model. The added first-order scavenging parameterization significantly improves the ^{7}Be and ^{210}Pb concentrations in the tropics and also improves $\gamma(^{7}\text{Be}/^{210}\text{Pb})$ slightly (Table 1). Increasing convective scavenging further would improve model agreement in the tropics but would be detrimental at higher latitudes. The persistently high values of the ratio suggest that part of the discrepancy for ^{7}Be is due to excessive transport to the surface. Independent evidence indicates that the GISS GCM 2 exaggerates the wet convective upward fluxes (and hence the compensating large-scale subsidence) in tropical regions [*Del Genio and Yao*, 1993]. A recent intercomparison of ^{222}Rn simulations in 10 established global three-dimensional models shows that ^{222}Rn concentrations in the upper troposphere in the GISS GCM 2 are high relative to other models [*Jacob et al.*, 1996]. Cloud entrainment, which is not included in this model, might also decrease $\gamma(^{7}\text{Be}/^{210}\text{Pb})$, since it is likely to increase ^{7}Be scavenging relative to ^{210}Pb.

At higher latitudes (> 20°), both ^{7}Be and ^{210}Pb are underestimated by the model in the northern hemisphere. Convective scavenging is also active at these latitudes, particularly in the summer. Therefore the added first-order convective scavenging has made the bias somewhat worse. The bias for the ratio is nearly zero at high latitudes for either parameterization. Low model ^{7}Be and ^{210}Pb surface concentrations resulting from excessive model rainfall, such as occurs over North America [*Hansen et al.*, 1983], are canceled by the ratio.

In Figure 7 we show observed and model ^{7}Be/^{210}Pb for surface concentrations and distinguish between low-elevation continental sites (asterisks) and remaining sites (crosses). The root mean square value for the concentration ratio is 6.4, compared with an average observed value of 6.6. Most of the spatial variability of the ratio results either because high-elevation sites have higher ^{7}Be concentration, or because distance from the ^{210}Pb contintental source produces low ^{210}Pb. Variability is low for the low-elevation continental sites north of about 25°S, which have ratios less than 12 (with an

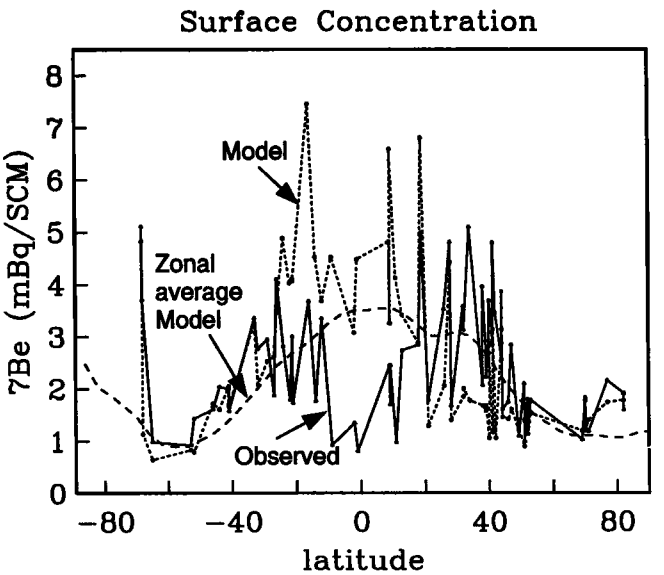

Figure 9. Observed (solid) and model (zonal average, long dashed; sites, short dashed) ^{7}Be surface concentrations (mBq/m^3 STP) as a function of latitude.

Table 1. Model Bias γ

	$\gamma(^7Be)$	$\gamma(^{210}Pb)$	$\gamma(^7Be/^{210}Pb)$
Updraft + first-order convective scavenging			
Tropics (< 20°)	0.990	0.210	0.370
High latitudes (> 20°)	-0.180	-0.300	-0.045
All sites	0.035	-0.250	0.037
Convective scavenging in updraft only			
Tropics (< 20°)	1.60	0.47	0.44
High latitudes (> 20°)	-0.06	-0.26	0.00
All sites	0.26	-0.19	0.10

Model bias γ as defined in equation (5), where γ=0 means zero bias, shown for the tropics, extratropics, and for all sites. The most southern Antarctic site was not included for calculations involving ^7Be, and Hawaii was not included for calculations involving ^{210}Pb since these misfits tend to dominate the bias.

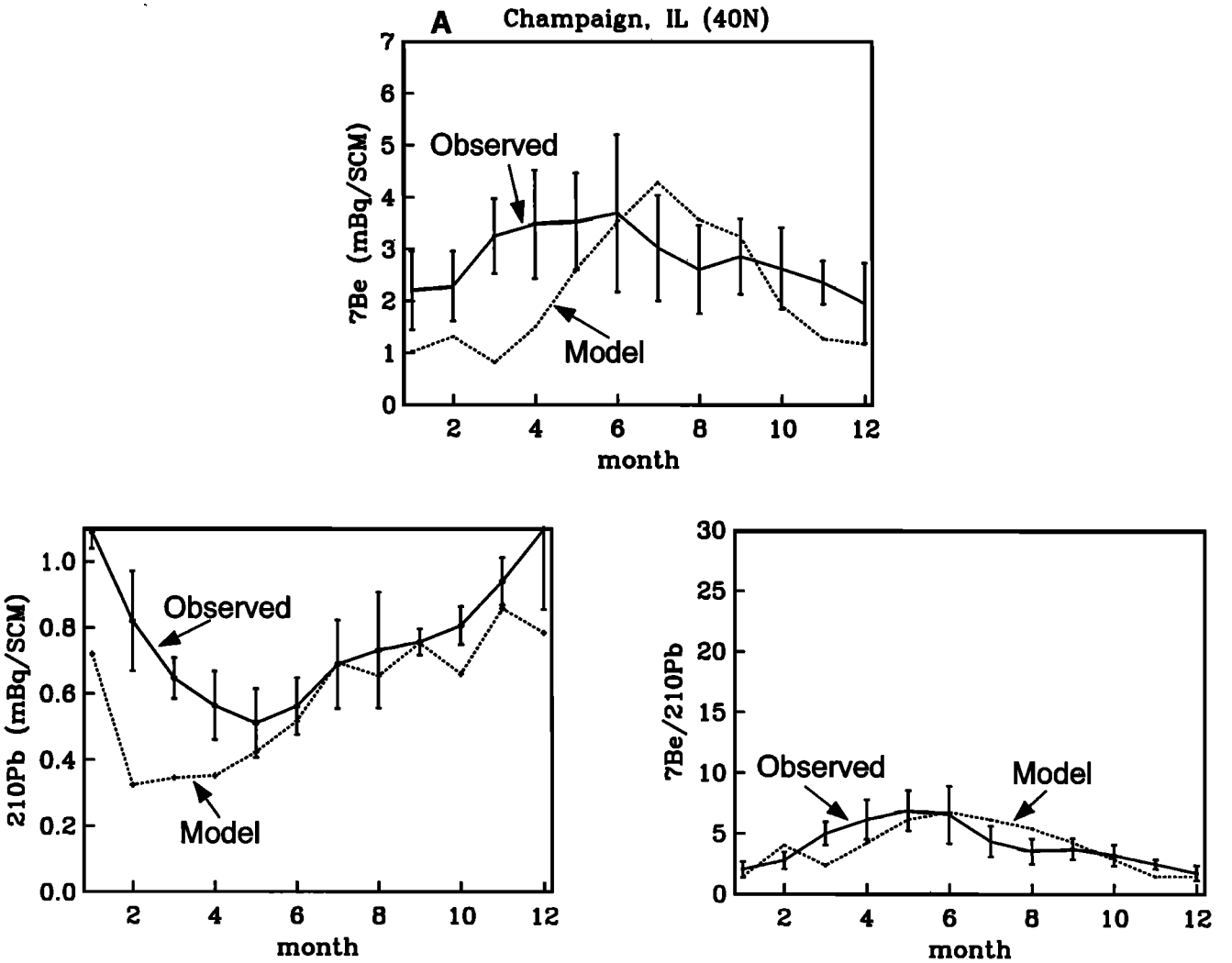

Figure 10. Seasonal variability of ^7Be (mBq/m^3 STP), ^{210}Pb (mBq/m^3 STP), and $^7Be/^{210}Pb$ (1-12 is January-December). Solid lines are observations, with standard deviations from the site's mean value, and dashed line is model. Sites are (a) Champaign, Illinois, (observations based on 53 months of ^7Be and ^{210}Pb data); (b) Santiago, Chile (based on 231 and 53 months of ^7Be and ^{210}Pb data, respectively); (c) Kap Tobin, Greenland (using 78 and 26 months of ^7Be and ^{210}Pb data, respectively); (d) Guayaquil, Ecuador (using 250 and 61 months of ^7Be and ^{210}Pb data, respectively).

average of about 6). Farther south the continental sites have higher ratios due to the weaker ^{210}Pb source. The midlatitude peaks observed for ^{7}Be in Figure 9 are removed in the ratio because of coincidence of high values for both ^{210}Pb and ^{7}Be over land.

In contrast with the spatial variability of the annual average ratio, the seasonal variability of ^{7}Be/^{210}Pb at individual sites is very large. Typically, the observed (monthly average) ratio varies by a factor of about 3 during the year at northern hemisphere continental sites and is as high as 6 or 7 over the southern hemisphere continents. We have compared observed and modeled seasonality at 46 sites and discuss here four examples which typify the dominant global trends. Since we are interested in exploring the utility of the ratio ^{7}Be/^{210}Pb as a diagnostic of vertical transport, we limit ourselves to continental sites. There is no typical behavior at ocean sites because of the large dependence of ^{210}Pb on lateral transport from its source.

Figure 10a shows ^{7}Be, ^{210}Pb, and ^{7}Be/^{210}Pb at Champaign, Illinois, which demonstrates typical midlatitude, continental behavior. Summertime convective mixing results in high ^{7}Be and low ^{210}Pb, while low-level stratification produces high ^{210}Pb during the winter. Although the model captures this seasonality, excess GCM precipitation during the winter causes both ^{7}Be and ^{210}Pb to be underestimated [*Hansen et al.*, 1983]. The good agreement between model and observed ^{7}Be/^{210}Pb ratio confirms this.

Santiago, Chile, Figure 10b, shows a southern hemisphere example of the same phenomena in the observations: minimum ^{210}Pb and maximum ^{7}Be are observed during the summer. Although the model captures the seasonality, it does not reproduce the very large values of ^{7}Be/^{210}Pb observed during the summer.

Kap Tobin, Greenland, Figure 10c, is an example of a site where ^{7}Be and ^{210}Pb have similar histories, as both are transported from lower latitudes during the winter (along with the "Arctic haze"). They are observed and modeled to be nearly in phase with each other, and both have maximum concentrations during the winter and spring. Therefore there is little seasonal variability in the ^{7}Be/^{210}Pb ratio. Excessive precipitation in the GCM Arctic winter causes ^{210}Pb and ^{7}Be to be underestimated (B93), while the ratio is well simulated.

Guayaquil, Ecuador, Figure 10d, illustrates the previ-

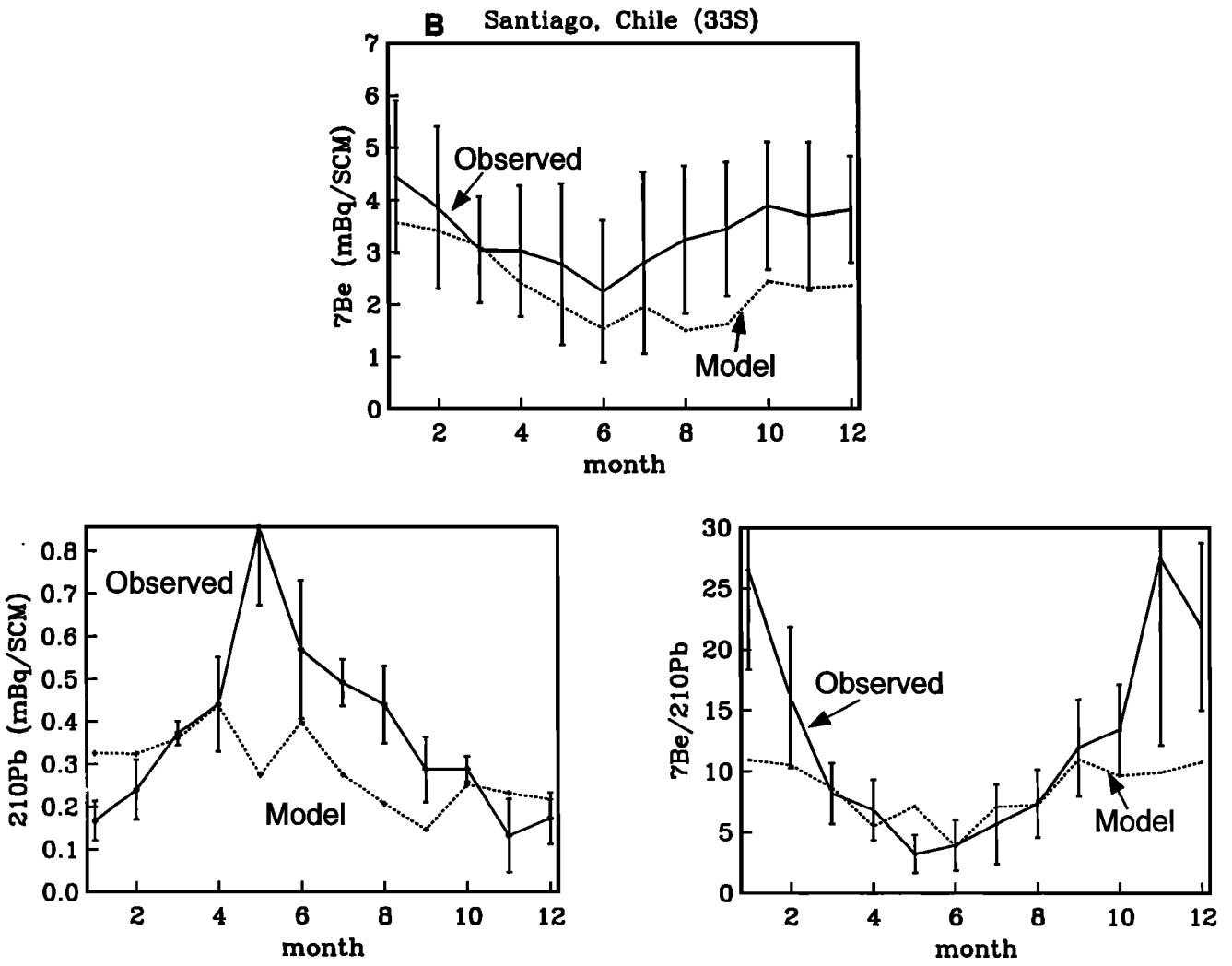

Figure 10. (continued)

ously discussed GCM flaws in simulating tropical convection. Both ^{7}Be and the $^{7}Be/^{210}Pb$ ratio are high. The GCM also does not accurately simulate the seasonal motion of the intertropical convergence zone, which is shifted too far north during the summer. Thus the seasonality of rainfall in the tropics is generally not correct.

Discussion

Ratio $^{7}Be/^{210}Pb$

In the previous section we showed that $^{7}Be/^{210}Pb$ is a sensitive tracer of vertical transport. Here we use model results to highlight some general properties of this tracer.

Figures 11 and 12 show the annual average model ratio of $^{7}Be/^{210}Pb$ for the deposition flux and surface concentration, respectively. Both figures show nearly constant values of $^{7}Be/^{210}Pb$ over the continents, with higher values away from the ^{210}Pb source. High-elevation regions also have higher $^{7}Be/^{210}Pb$ concentrations. The ratio between Figure 11 (the deposition flux ratio) and Figure 12 (the surface concentration) has a slight positive poleward gradient, so that the deposition flux ratio increases toward the poles faster than does the surface concentration ratio. The reason for this is shown in Figure 13, the annual average zonal average ratio. The smallest vertical gradient occurs near the equator, where convective mixing generates a nearly constant ratio value of about $^{7}Be/^{210}Pb = 20$. At higher latitudes, $^{7}Be/^{210}Pb$ increases with altitude. Since precipitation scavenges air aloft, the poleward gradient of the ratio is greater for the deposition flux than the surface air concentration. There is little seasonal variability in the zonal average concentration ratio. At altitudes above about 600 mbar the $^{7}Be/^{210}Pb$ gradient increases more gradually in the summer, both because ^{210}Pb is mixed upward more readily during the summer (B93) and because the high-altitude subsidence of ^{7}Be is greater during the winter, as we will discuss below. Note the sharp increase of $^{7}Be/^{210}Pb$ toward the south pole. We said that the model does not attain sufficiently high values of $^{7}Be/^{210}Pb$ during the summer in the southern hemisphere. This may result either from insufficient vertical mixing or from a slight displacement in the southern hemisphere north-south $^{7}Be/^{210}Pb$ gradient.

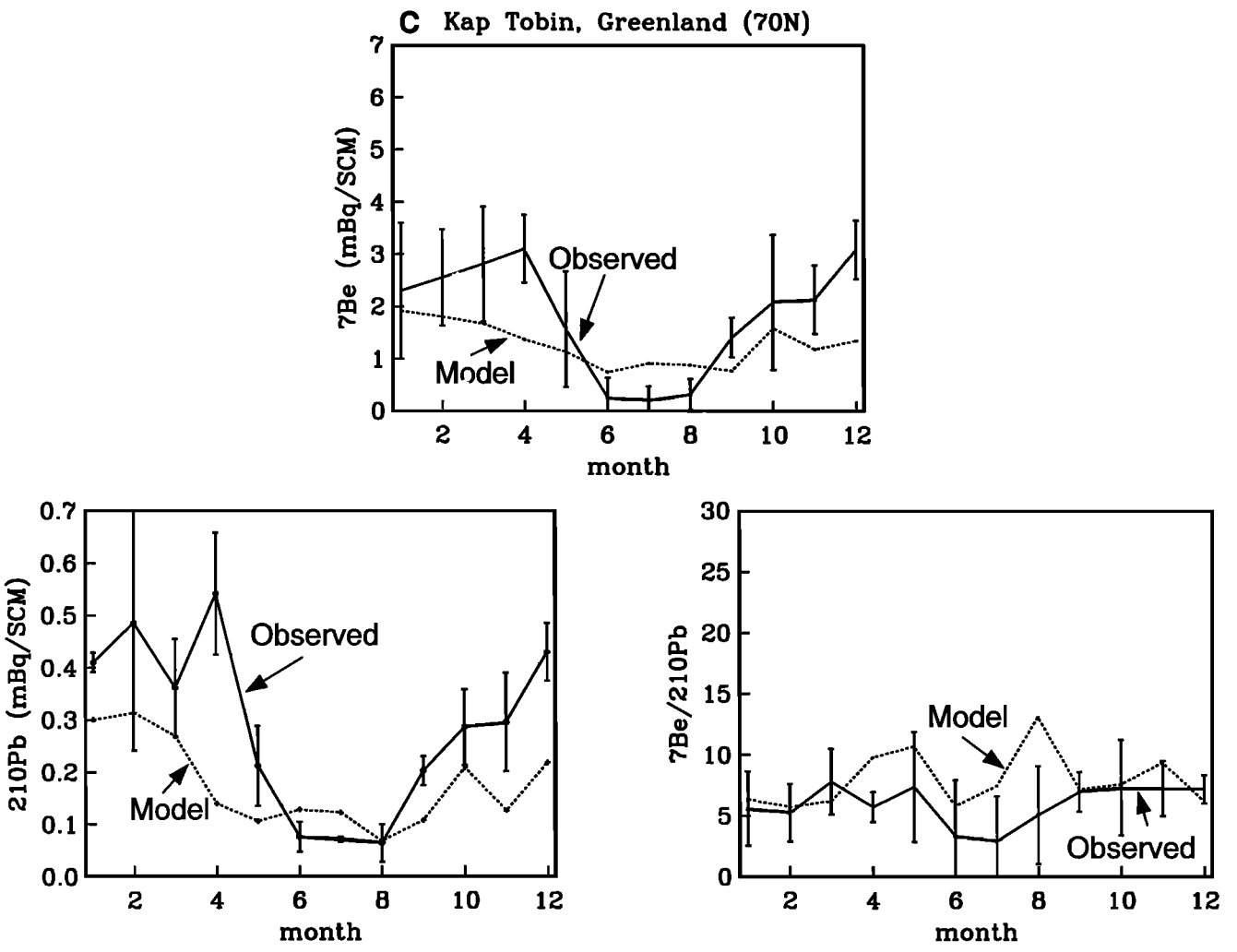

Figure 10. (continued)

We showed in the previous section that the seasonal variability of $^{7}Be/^{210}Pb$ is much larger than the spatial variability of the annual average ratio and that the model simulation of the ratio seasonality over land was fairly accurate. Figure 14 shows the $^{7}Be/^{210}Pb$ surface concentration ratio in January and July, normalized by the annual average ratio calculated at each grid box. This normalization removes variability associated with the radionuclide sources. Figure 14 demonstrates the large variability in vertical exchange with the surface which occurs during the year due to (primarily dry) convection. As already noted, highest values of $^{7}Be/^{210}Pb$ (>1 in Figure 14) over continents occur during the summers. These regions correlate with dry convection in the GCM. The ratio is also high over certain oceanic regions during the winter. Many of these regions (e.g., the Norwegian Sea in January and south of South America in July) correlate with both dry and wet convection in the GCM. The absolute amplitude of variability in the model is typically lower over the oceans; however, these plots do not show this because of the normalization.

Although not shown here, we have also examined the seasonality of the $^{7}Be/^{210}Pb$ deposition flux. In general, the $^{7}Be/^{210}Pb$ deposition flux is higher over the winter hemisphere, over both oceans and continents. This may be related to the increased flux of ^{7}Be from the stratosphere during the winter. However, in many regions the wintertime high ratio deposition flux is correlated with model convection. There is also no apparent correlation between surface concentration ratio or deposition flux ratio and model high-pressure regions. This model therefore suggests that maximum input of ^{7}Be from the stratosphere and downwelling in the Hadley circulation occur during the winter and spring but that convective activity retains a crucial role for generating high values of ^{7}Be and $^{7}Be/^{210}Pb$ in deposition flux as well as surface concentrations.

Aerosol Residence Times

Removal of ^{7}Be and ^{210}Pb from the troposphere in the model is dominated by convective precipitation scavenging. This may be accentuated because the GCM has excessive convective precipitation relative to large-scale precipitation at high latitudes [*Del Genio et al.*, 1996]. Lead 210 is removed almost entirely by deposition: 81% by convective precipitation, 7% by large scale precipitation, and 12% by dry deposition. Since ^{7}Be has a 53-day half-life, and has high concentrations in the up-

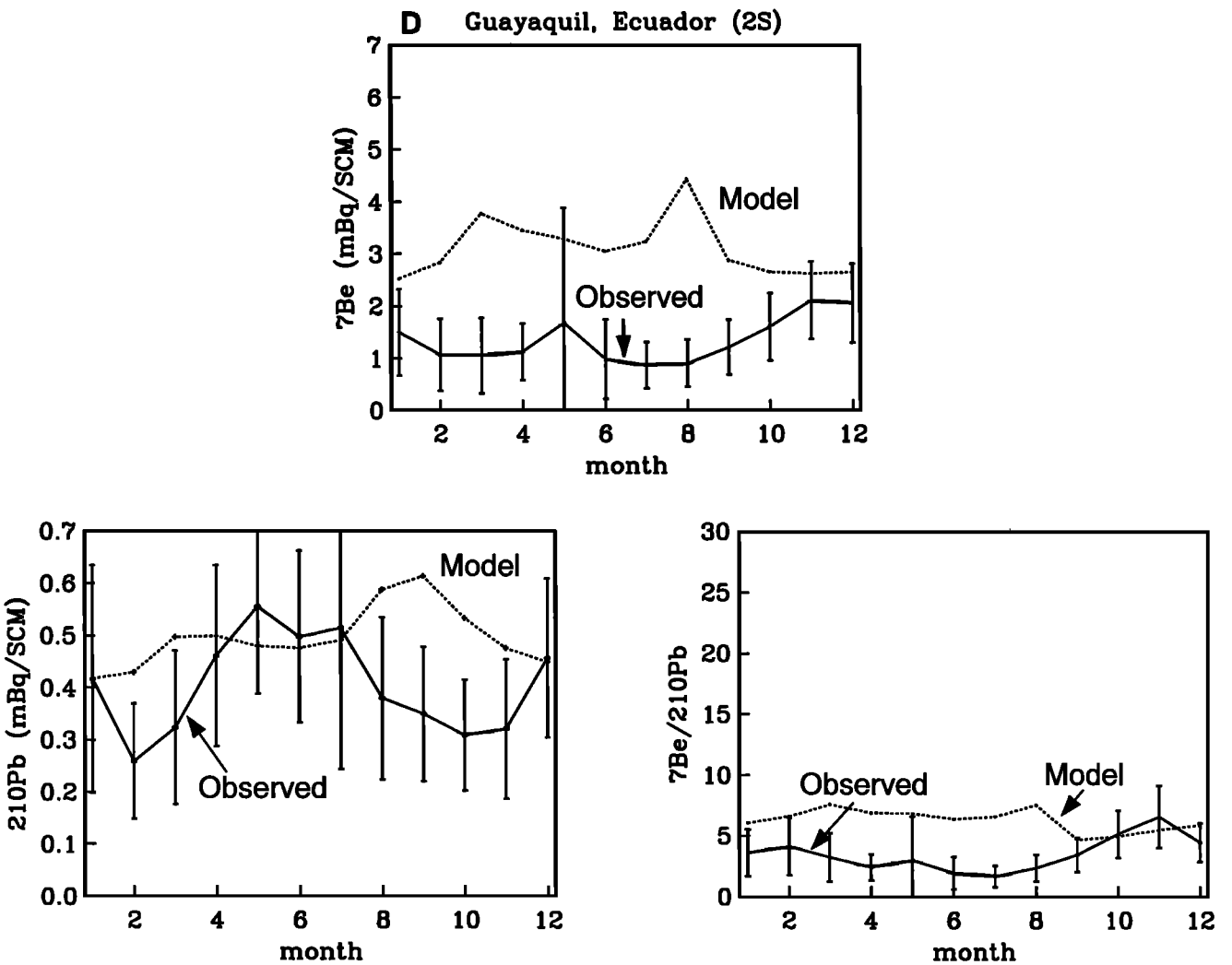

Figure 10. (continued)

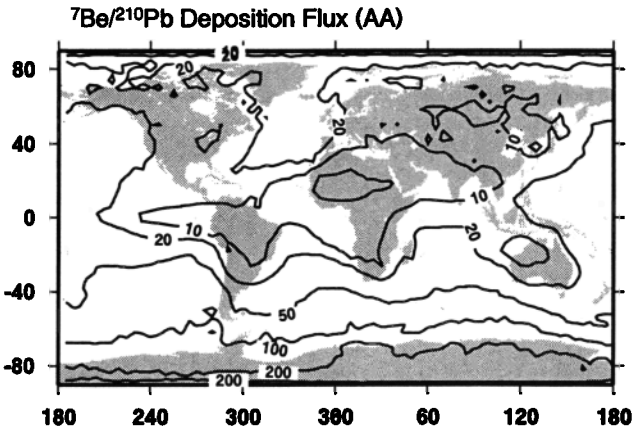

Figure 11. Model annual average $^{7}Be/^{210}Pb$ deposition flux. Contours shown are 2, 5, 10, 20, 50, 100, 200.

per troposphere, some tropospheric removal occurs by decay. Seventy-one percent of the removal from the troposphere is by deposition: 63% by convective precipitation, 5% by large-scale precipitation, and 3% by dry deposition. The remaining tropospheric loss, 29%, is by radioactive decay.

Figure 15 shows the annual average tropospheric residence time τ of ^{7}Be and ^{210}Pb as a function of latitude, where $\tau = C/\Phi$, C is the tropospheric column, and Φ is the total deposition flux at that latitude. The residence times for ^{7}Be are larger than for ^{210}Pb, since the distribution of the former is weighted toward the upper troposphere where precipitation is infrequent. Global tropospheric residence times are 21 days for ^{7}Be and 9 days for ^{210}Pb. The values are most similar in the tropics where convective mixing and precipitation affects both radionuclides similarly. This is aided by the convective pumping of radon, the gaseous precursor to ^{210}Pb, to high altitudes (B93). The dry subtropics and polar regions have relatively long residence times. The ^{7}Be results agree with those of *Bleichrodt* [1978], who calculated a ^{7}Be residence time between 22 and 35 days

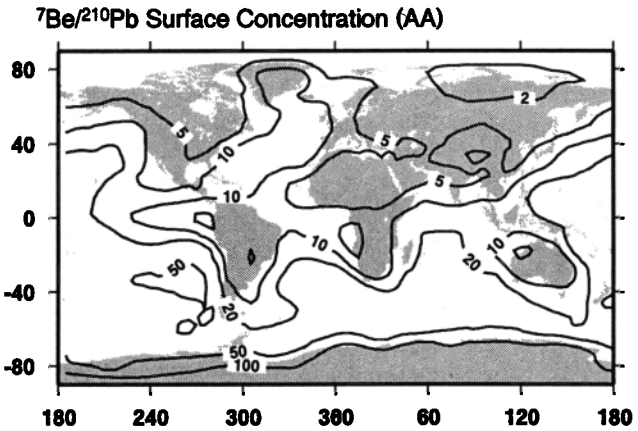

Figure 12. Model annual average $^{7}Be/^{210}Pb$ surface concentration ratio. Contours shown are the same as in figure 11.

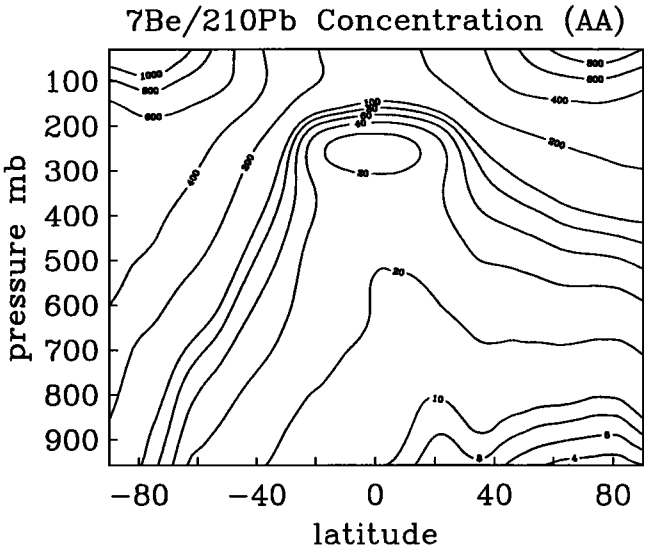

Figure 13. Model zonal, annual average $^{7}Be/^{210}Pb$ concentration ratio.

at northern midlatitudes (30°-75°N), using observed deposition fluxes and air concentrations at those latitudes.

Comparison With Previous Modeling

We compare some aspects of the GISS CTM results for ^{7}Be with the ECMWF results of *Brost et al.* [1991] (using ECHAM2) and *Rehfeld and Heimann* [1995]. *Brost et al.* [1991] also had problems with overpredicting ^{7}Be concentrations in the tropics (typically by about 100%). *Rehfeld and Heimann* [1995] were more successful at capturing the observed tropical minimum in ^{7}Be concentrations.

Rehfeld and Heimann [1995] have (≈50%) higher ^{7}Be surface concentrations over continents in the subtropics during the winter. Their ^{210}Pb residence times in the subtropics are also much greater (≈25-30 days) than that calculated by B93 (≈12-15 days), although in other regions the ^{210}Pb residence times are comparable. *Rehfeld* [1994] also considered the ratio $^{7}Be/^{210}Pb$. His results are qualitatively similar to ours; however, his annual average concentration ratio does not have the noticeable minima over continents that ours does, particularly in the northern hemisphere.

Brost et al. [1991] did not account for the effect of the solar cycle, although they used the LP67 source based on the 1958 solar maximum year. Had they corrected the data, the ^{7}Be model results would have been at least 20% high relative to observations. *Rehfeld and Heimann* [1995] also used LP67 but minimized this problem by working with observations from the year 1990 only, a year of maximum solar activity.

A final point of comparison is a difference in ^{7}Be tropospheric radioactive decay. While we found about 29% of ^{7}Be removal was from decay, *Brost et al.* [1991] reported this loss to be "trivial" in their model. Unfortunately, neither they nor *Rehfeld and Heimann* [1995] reported model ^{7}Be residence times, limiting further comparison of aerosol lifetimes between models.

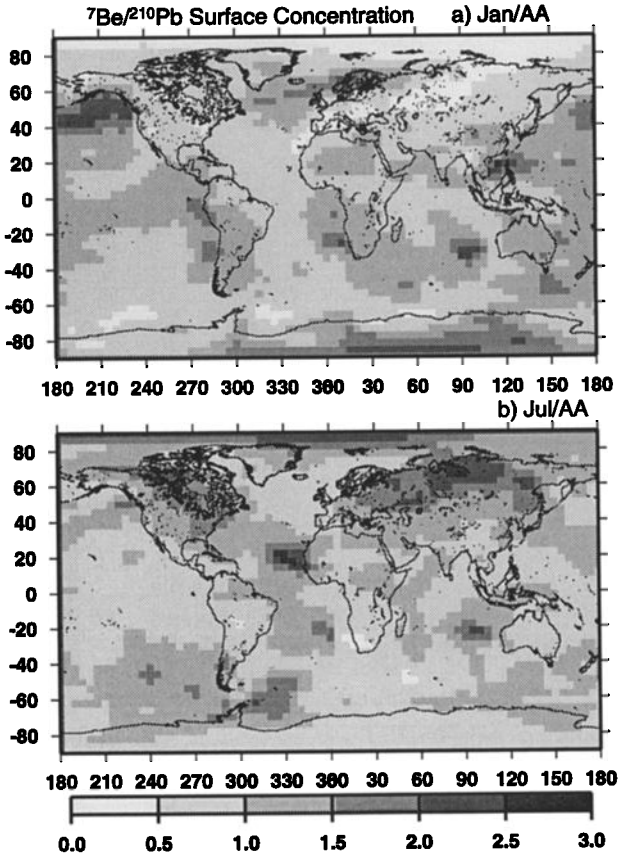

Figure 14. Model $^{7}Be/^{210}Pb$ surface concentration ratio: (a) January and (b) July normalized in each case by the local annual average surface concentration ratio (Figure 12).

Conclusions

The aerosol tracers ^{7}Be and ^{210}Pb, taken together, offer an excellent test for the simulation of vertical transport and aerosol scavenging in global models. The ratio $^{7}Be/^{210}Pb$ enables distinction between precipitation errors and other errors and provides a particularly sensitive measure of vertical transport. Application to the GISS GCM 2 [*Hansen et al.*, 1983] shows that a convective scavenging parameterization previously tested by simulation of ^{210}Pb failed to remove enough ^{7}Be. It is therefore important to consider the downward convective transport and scavenging of species with a high-altitude source, such as ^{7}Be, in addition to the transport and scavenging of a surface-derived species such as ^{210}Pb.

To correct for insufficient ^{7}Be scavenging and high ^{7}Be surface concentrations in the tropics, we added a first-order scavenging parameterization to the convective scavenging in the updrafts. This compensates for the absence of cloud entrainment and of precipitation from the cloud anvil. The persistence of high ^{7}Be after the additional scavenging indicates excessive deep convective mass fluxes in the GISS GCM 2. Preliminary

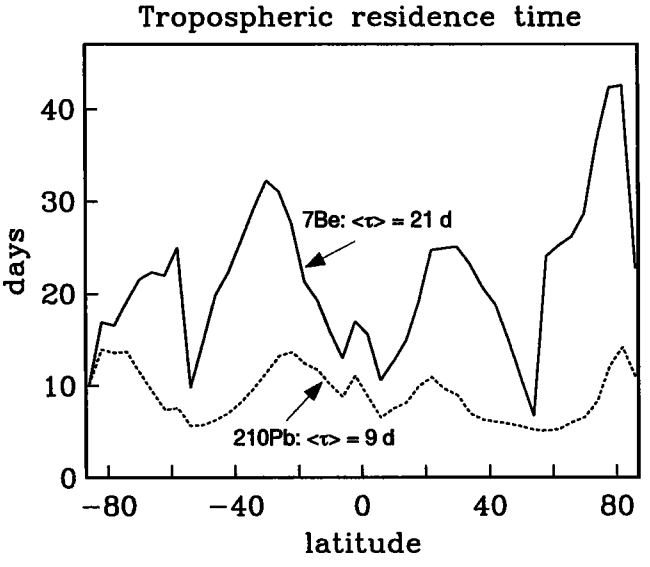

Figure 15. Zonally averaged, annual mean tropospheric residence times of ^{7}Be (solid) and ^{210}Pb (dashed) as a function of latitude.

^{7}Be simulations using the new generation GISS GCM 2 prime [*Rind and Lerner*, 1996], including an improved wet convection scheme [*Del Genio and Yao*, 1993; *Del Genio et al.*, 1996], indicate considerable amelioration in the ability of the model to match observations.

Although the model is limited partly by GCM precipitation anomalies [*Hansen et al.*, 1983] in its ability to simulate ^{7}Be, ^{210}Pb, or other aerosols, it is more successful at predicting the concentration ratio $^{7}Be/^{210}Pb$. In continental regions, $^{7}Be/^{210}Pb$ is an index of vertical mixing. The annual average spatial variability of $^{7}Be/^{210}Pb$ is small; however, the seasonal variability of the ratio at particular locations is large. The ratio is maximum over continents during the summer due to increased dry convective mixing. Although the model is less reliable over the oceans, it indicates certain regions of high $^{7}Be/^{210}Pb$ during the winter, both in the surface concentrations and in the deposition flux. These regions also tend to be correlated with convective activity in the model. The $^{7}Be/^{210}Pb$ deposition flux is somewhat higher over continents during the winter. This is likely a result of the increase in $^{7}Be/^{210}Pb$ at intermediate to high altitudes during the winter and spring as increased ^{7}Be enters from the stratosphere and convective pumping of ^{222}Rn is decreased. In summary, $^{7}Be/^{210}Pb$ indicates that large-scale transport, such as the Hadley circulation, is important for vertical mixing in the midtroposphere; however, convective transport is primarily responsible for delivering high-altitude ^{7}Be-rich air to the surface.

Acknowledgments. We thank Karl Turekian and two anonymous reviewers for insightful comments and criticisms. We thank Devandra Lal and Keran O'Brien for supplying their cosmogenic radionuclide sources. H. Wershofen provided data records from Physikalisch Technische Bundesanstalt and John Kada provided records from the En-

vironmental Measurements Laboratory. We thank Stefan Rehfeld for a copy of his PhD thesis. D. Koch is grateful to C. Spivakovsky, Y. Balkanski, G. Gardner and others in the Harvard atmospheric group for helpful discussions and assistance with the modeling work. Work at Yale was funded by DOE (DE-FG02-94ER61925), work at Harvard was funded by NASA (NASA-NAGW-2632 and Subsonic Assessment Program), and D. Koch was also supported by NASA's Atmospheric Chemistry Modeling and Analysis Program.

References

Balkanski, Y. J., D. J. Jacob, G. M. Gardner, W. C. Graustein, and K. K. Turekian, Transport and residence times of aerosols inferred from a global three-dimensional simulation of ^{210}Pb, *J. Geophys. Res.*, *98*, 20,573-20,586, 1993.

Baskaran, M., C. H. Coleman, and P. H. Santischi, Atmospheric depositional fluxes of ^{7}Be and ^{210}Pb at Galveston and College Station, Texas, *J. Geophys. Res.*, *98*, 20,555-20,571, 1993.

Bleichrodt, J. F., Mean tropospheric residence time of cosmic-ray-produced beryllium 7 at north temperate latitudes, *J. Geophys. Res.*, *83*, 3058-3062, 1978.

Brost, R. A., J. Feichter, and M. Heimann, Three-dimensional simulation of ^{7}Be in a global climate model, *J. Geophys. Res.*, *96*, 22,423-22,445, 1991.

Brown, L., G. J. Stensland, J. Klein, and R. Middleton, Atmospheric deposition of ^{7}Be and ^{210}Pb, *Geochem. Cosmochem. Acta*, *53*, 135-142, 1989.

Charlson, R. J., J. Langner, H. Rodhe, C. B. Leovy, and S. G. Warren, Perturbation of the northern hemisphere radiative balance by backscattering from anthropogenic sulfate aerosols, *Tellus*, *43AB*, 152-163, 1991.

Charlson, R. J., S. E. Schwartz, J. M. Hales, R. D. Cess, J. A. Coakley Jr., J. E. Hansen, and D. J. Hofmann, Climate forcing by anthropogenic aerosols, *Science*, *255*, 423-430, 1992.

Clarke, A. D., Atmospheric nuclei in the remote free troposphere, *J. Atmos. Chem.*, *14*, 479-488, 1992.

Crecelius, E. A., Prediction of marine atmospheric deposition rates using total ^{7}Be deposition velocities, *Atmos. Environ.*, *15*, 579-582, 1981.

Dana, M. T., and J. M. Hales, Statistical aspects of the washout of polydisperse aerosols, *Atmos. Environ.*, *10*, 45-50, 1976.

Davidson, C. I., Mechanisms of wet and dry deposition of atmospheric contaminants to snow surfaces, in *The Environmental Record in Glaciers and Ice Sheets*, edited by H. Oeschger and C. C. Langway Jr., pp. 29-51, John Wiley, 1989.

Del Genio, A. D., and M.-S. Yao, Efficient cumulus parameterization for long-term climate studies: The GISS scheme, in *The Representation of Cumulus Convection in Numerical Models*, edited by K. A. Emanuel and D. J. Raymond, Am. Meteorol. Soc. Monogr., *46*, 181-184, 1993.

Del Genio, A. D., M.-S. Yao, W. Kovari, and K. K.-W. Lo, A prognostic cloud water parameterization for global climate models, *J. Clim.*, *9*, 270-304, 1996.

Dibb, J. E., Atmospheric deposition of beryllium 7 in the Chesapeake Bay region, *J. Geophys. Res.*, *94*, 2261-2265, 1989.

Dibb, J. E., R. W. Talbot, and G. L. Gregory, Beryllium 7 and lead 210 in the western hemisphere Arctic atmosphere: Observations from three recent aircraft-based sampling programs, *J. Geophys. Res.*, *97*, 16,709-16,715, 1992.

Dibb, J. E., L. D. Meeker, R. C. Finkel, J. R. Southon, M. W. Caffee, and L. A. Barrie, Estimation of stratospheric input to the Arctic troposphere: ^{7}Be and ^{10}Be in aerosols at Alert, Canada, *J. Geophys. Res.*, *99*, 12,855-12,864, 1994.

Dutkiewicz, V. A., and L. Husain, Stratospheric and tropospheric components of ^{7}Be in surface air, *J. Geophys. Res.*, *90*, 5783-5788, 1985.

Feely, H. W., L. Toonkel, and R. J. Larsen, Radionuclides and trace elements in surface air, *EML-Rep.-395*, Environ. Meas. Lab., Dep. of Energy, New York, 1981.

Feely, H. W., R. J. Larsen, and C. G. Sanderson, Annual report of the surface air sampling program, *EML-Rep.-440*, Environ. Meas. Lab., Dep. of Energy, New York, 1985.

Feely, H. W., R. J. Larsen, and C. G. Sanderson, Annual report of the surface air sampling program, *EML-Rep.-497*, Environ. Meas. Lab., Dep. of Energy, New York, 1988.

Feichter, J., R. A. Brost, and M. Heimann, Three-dimensional modeling of the concentration and deposition of ^{210}Pb aerosols, *J. Geophys. Res.*, *96*, 22,447-22,460, 1991.

Giorgi, F., and W. L. Chameides, Rainout lifetimes of highly soluble aerosols and gases as inferred from simulations with a general circulation model, *J. Geophys. Res.*, *91*, 14,367-14,376, 1986.

Hansen, J., G. Russell, D. Rind, P. Stone, A. Lacis, S. Lebedeff, R. Ruedy, and L. Travis, Efficient three-dimensional global models for climate studies: Models I and II, *Mon. Weather Rev.*, *111*, 609-662, 1983.

Hasebe, N., T. Doke, J. Kikuchi, Y. Takeuchi, and T. Sugiyama, Observation of fallout rates of atmospheric ^{7}Be and ^{22}Na produced by cosmic rays concerning estimation of the fallout rate of atmospheric ^{26}Al, *J. Geophys. Res.*, *86*, 520-524, 1981.

Jacob, D. J., et al., Evaluation and intercomparison of global atmospheric transport models using ^{222}Rn and other short-lived tracers, *J. Geophys. Res.*, in press, 1996.

Knies, D. L., Cosmogenic radionuclides in precipitation, Ph.D. dissertation, Purdue Univ., West Lafayette, Ind., 1994.

Koch, D. M., and M. E. Mann, Spatial and temporal variability of ^{7}Be surface concentrations, *Tellus*, in press, 1996.

Kolb, W., Aktivitatskonzentrationen von Radionukliden in der bodennahen Luft Norddeutschlands und Nordnorwegens im Zeitraum von 1963 bis 1990, *PTB-Ber. Ra-29, Phys.-Tech. Bundesanst.*, Braunschweig, Germany, 1992.

Kritz, M. A., S. W. Rosner, E. F. Danielsen, and H. B. Selkirk, Air mass origins and troposphere-to-stratosphere exchange associated with midlatitude cyclogenesis and tropopause folding inferred from ^{7}Be measurements, *J. Geophys. Res.*, *96*, 17,405-17,414, 1991.

Lal, D., and B. Peters, Cosmic ray produced radioactivity on the Earth, *Hand. Phys*, *46*, 551-612, 1967.

Lal, D., V. N. Nijampurkar, G. Rajagopalan, and B. L. K. Somayajulu, Annual fallout of ^{32}Si, ^{210}Pb, ^{22}Na, ^{35}S and ^{7}Be in rains in India, *Proc. Ind. Acad. Sci.*, *88*, 29-40, 1979.

Lambert, G., B. Ardouin, and J. Sanak, Atmospheric transport of trace elements toward Antarctica, *Tellus*, *42B*, 76-82, 1990.

Larsen, R. J., and C. G. Sanderson, Annual report of the surface air sampling program, *EML-Rep.-524*, Environ. Meas. Lab., Dep. of Energy, New York, 1990.

Larsen, R. J., and C. G. Sanderson, Annual report of the surface air sampling program, *EML-Rep.-541*, Environ. Meas. Lab., Dep. of Energy, New York, 1991.

Leifer, R. ,and Z. R. Juzdan, The high altitude sampling program: Radioactivity in the stratosphere, final report, December 1986, *EML-Rep.-458*, Environ. Meas. Lab., Dep. of Energy, New York, 1986.

Marenco, A., and J. Fontan, Etude des variations des ^{7}Be, ^{32}P, ^{90}Sr, ^{210}Pb et ^{210}Po dans la troposphere, *Tellus*, *26*, 386-401, 1974.

O'Brien, K., Secular variations in the production of cosmogenic isotopes in the Earth's atmosphere, *J. Geophys. Res.*, *84*, 423-431, 1979.

O'Brien, K., A. De La Zerda Lerner, M. A. Shea, and D. F. Smart, The production of cosmogenic isotopes in the Earth's atmosphere and their inventories, in *The Sun in Time*, pp. 317-342, Univ. of Arizona Press, Tucson, 1991.

Olsen, C. R., I. L. Larsen, P. D. Lowry, N. H. Cutshall, J. F. Todd, G. T. F. Wong, and W. H. Casey, Atmospheric fluxes and marsh-soil inventories of ^{7}Be and ^{210}Pb, *J. Geophys. Res.*, *90*, 10,487-10,495, 1985.

Parker, R. P., Beryllium-7 and fission products in surface air, *Nature*, *193*, 967-968, 1962.

Prather, M. J., Numerical advection by conservation of second-order moments, *J. Geophys. Res.*, *91*, 6671-6681, 1986.

Prather, M., M. M. McElroy, S. Wofsy, G. Russell, and D. Rind, Chemistry of the global troposphere: Fluorocarbons as tracers of air motion, *J. Geophys. Res.*, *92*, 6579-6613, 1987.

Rangarajan, C., and C. D. Eapen, The use of natural radioactive tracers in a study of atmospheric residence times, *Tellus*, *42B*, 142-147, 1990.

Rangarajan, C., and S. Gopalakrishnan, Seasonal variation of beryllium 7 relative to caesium-137 in surface air at tropical and sub-tropical latitudes, *Tellus*, *22*, 115-120, 1970.

Rehfeld, S., Deposition radioacktiver Tracer in einem Transportmodell der Atmosphäre, Ph.D. dissertation, Max-Planck-Inst. für Meteorol., Hamburg, Germany, 1994.

Rehfeld, S., and M. Heimann, Three dimensional atmospheric transport simulation of the radioactive tracers ^{210}Pb, ^{7}Be, ^{10}Be, and ^{90}Sr, *J. Geophys. Res.*, *100*, 26,141-26,161, 1995.

Rind, D., and J. Lerner, The use of on-line tracers as a diagnostic tool in GCM model development, *J. Geophys. Res.*, in press, 1996.

Rodhe, H., Precipitation scavenging and tropospheric mixing, in *Precipitation Scavenging, Dry Deposition and Resuspension*, Elsevier, New York, 1983.

Sanak, J., G. Lambert, and B. Ardouin, Measurements of stratosphere-to-troposphere exchange in Antarctica by using short-lived cosmonuclides, *Tellus*, *37B*, 109-115, 1985.

Shapiro, M. H., and J. L. Forbes-Resha, Mean residence time of ^{7}Be-bearing aerosols in the troposphere, *J. Geophys. Res.*, *81*, 2647-2649, 1976.

Schumann, G., and M. Stoeppler, Beryllium 7 in the atmosphere, *J. Geophys. Res.*, *68*, 3827-3830, 1963.

Tanaka, N. and K. K. Turekian, Determination of the dry deposition flux of SO_2 using cosmogenic ^{35}S and ^{7}Be measurements, *J. Geophys. Res.*, *100*, 2841-2848, 1995.

Todd, J. F., G. T. F. Wong, C. R. Olsen, and I. L. Larsen, Atmospheric depositional characteristics of beryllium 7 and lead 210 along the southeastern Virginia coast, *J. Geophys. Res.*, *94*, 11,106-11,116, 1989.

Turekian, K. K., L. K. Benninger, and E. P. Dion, ^{7}Be and ^{210}Pb total deposition fluxes at New Haven, Connecticut, and at Bermuda, *J. Geophys. Res.*, *88*, 5411-5415, 1983.

Uematsu, M., R. A. Duce, and J. M. Prospero, Atmospheric beryllium 7 concentrations over the Pacific Ocean, *Geophys. Res. Lett.*, *21*, 561-564, 1994.

Viezee, W., and W. B. Singh, The distribution of beryllium 7 in the troposphere: Implications on stratosphere/troposphere exchange, *Geophys. Res. Lett.*, *7*, 805-808, 1980.

Young, J. A., and W. B. Silker, Aerosol deposition velocities on the Pacific and Atlantic Oceans calculated from ^{7}Be measurements, *Earth and Planet. Sci. Lett.*, *50*, 92-104, 1980.

W.C. Graustein, Department of Geology and Geophysics, Yale University, P.O. Box 208109, New Haven, CT 06520-8109.

D.J. Jacob, Department of Earth and Planetary Sciences, Harvard University, Pierce Hall, 29 Oxford Street, Cambridge, MA 02138.

D.M. Koch, Columbia University, Goddard Institute for Space Studies, 2880 Broadway, New York, NY 10025. (e-mail: koch@thebes.giss.nasa.gov)

(Received May 18, 1995; revised March 11, 1996; accepted March 13, 1996.)